

---

This is an electronic reprint of the original article.  
This reprint may differ from the original in pagination and typographic detail.

Author(s): Cingolani, R. & Rinaldi, R. & Lipsanen, Harri & Sopenen, M. & Virkkala, R. & Majjala, K. & Tulkki, J. & Ahopelto, J. & Uchida, K. & Miura, N. & Arakawa, Y.

Title: Electron-Hole Correlation in Quantum Dots under a High Magnetic Field (up to 45 T)

Year: 1999

Version: Final published version

**Please cite the original version:**

Cingolani, R. & Rinaldi, R. & Lipsanen, Harri & Sopenen, M. & Virkkala, R. & Majjala, K. & Tulkki, J. & Ahopelto, J. & Uchida, K. & Miura, N. & Arakawa, Y. 1999. Electron-Hole Correlation in Quantum Dots under a High Magnetic Field (up to 45 T). Phys. Rev. Lett. Volume 83, Issue 23. P. 4832-4835. ISSN 0031-9007 (printed). DOI: 10.1103/physrevlett.83.4832.

Rights: © 1999 American Physical Society (APS). <http://www.aps.org/>

---

All material supplied via Aaltodoc is protected by copyright and other intellectual property rights, and duplication or sale of all or part of any of the repository collections is not permitted, except that material may be duplicated by you for your research use or educational purposes in electronic or print form. You must obtain permission for any other use. Electronic or print copies may not be offered, whether for sale or otherwise to anyone who is not an authorised user.

## Electron-Hole Correlation in Quantum Dots under a High Magnetic Field (up to 45 T)

R. Cingolani and R. Rinaldi

*INFN-Lecce, Dipartimento Ingegneria dell'Innovazione, Universita' di Lecce, via Arnesano, 73100 Lecce, Italy*

H. Lipsanen and M. Sopanen

*Optoelectronics Laboratory, Helsinki University of Technology, Otakaari 7A, P.O. Box 3000, FIN-02015 HUT, Finland*

R. Virkkala, K. Majjala, and J. Tulkki

*Laboratory of Computational Engineering, Helsinki University of Technology, Miestentie 3, P.O. Box 9400, FIN-02015 HUT, Finland*

J. Ahopelto

*VTT Electronics, Tekniikantie 17, P.O. Box 1101 FIN-02044 VTT, Finland*

K. Uchida and N. Miura

*MegaGauss Laboratory, Institute for Solid State Physics, University of Tokyo, Minato-ku, Japan*

Y. Arakawa

*Institute of Industrial Science, University of Tokyo, Japan*

(Received 21 May 1999)

The influence of the direct and exchange Coulomb interaction on Landau level formation in strain induced quantum dots has been studied by high-field (45 T) magnetoluminescence and by many-electron many-hole Hartree-Fock calculations. The Darwin Fock states of the dots are found to merge into a unique Landau level at very high fields with a considerable reduction in the total diamagnetic shift due to the enhanced electron-hole correlation caused by the increased degeneracy of the state. We calculate a 50% reduction of the diamagnetic shift as a result of direct and exchange Coulomb interaction in the squeezed carrier states, in excellent agreement with the experimental findings.

PACS numbers: 71.70.Ej, 73.20.Dx, 78.55.Cr

Recently, it has been demonstrated [1] that the magnetic interaction in quantum dots (QD) with axially symmetric potential causes the lifting of the degeneracy of states having different values of the angular momentum quantum number [2,3]. The resulting Zeeman splitting, observed in the QD luminescence spectra, is related to the mesoscopic magnetic momentum of electrons and holes which overwhelms the spin splitting. This picture is well reproduced by single particle Luttinger-Kohn calculations in the low-field limit (below 10 T). At high fields, the shrinkage of the carrier wave functions in the dots and the increased degeneracy of the electronic levels lead to a strong enhancement of the electron-electron and electron-hole correlation. Therefore, the spectroscopic investigation of the optical transition of strongly confined quantum dots in very high magnetic field becomes a unique tool for the direct measure of the electron-hole correlation energy in artificial atoms.

To this aim we have studied both experimentally and theoretically the magnetoluminescence spectra of InGaAs strain induced quantum dots under optical excitation in the range 0–45 T. Our dots are strongly confined (typical intersubband splitting in the range of 15 meV), and neutral, so that a direct measure of the electron-hole correlation is obtained optically and at normal cryogenic

temperatures (4 K), as opposed to other pioneering papers in which the experiments were conducted well below 1 K and in charged dots [4,5]. The electron-hole correlation is found to reduce the diamagnetic shift of the lowest quantum dot Landau levels by over 20 meV at 40 T. Furthermore, a suppression of the state filling and a strong transfer of carriers from the high energy quantum dot Darwin-Fock states into the ground state of the quantum well is observed at fields higher than 20 T. Our theory predicts—in excellent agreement with the experiments—that when the zero field QD electron and hole states merge into the electron and hole Landau levels, the increased degeneracy of the electron and hole states allows for increasingly many electrons and holes to occupy the lowest energy level. This is seen in the luminescence spectrum as a gradual increase of the QD ground state luminescence while the excited state luminescence lines fade out at high fields. As a main consequence the  $e$ - $h$  correlation increases with increasing the magnetic field and thus the comparison between theory and experiment provides the first determination of such electron-hole correlation energy in neutral dots.

The investigated samples were grown by metal-organic vapor phase epitaxy at atmospheric pressure. The QD consist of a 8 nm thick  $\text{In}_{0.2}\text{Ga}_{0.8}\text{As}$  quantum well (QW)

buried by a GaAs barrier of thickness 5 nm. Self-organized InP islands (stressors) are grown on the GaAs surface in order to induce a paraboliclike strain potential which laterally confines the carriers in the InGaAs QW underneath the stressor. Details on the samples can be found in Ref. [6]. The magnetoluminescence measurements were performed by inserting the sample in a pulsed-resistive magnet, operating between 0 and 45 T, at 4 K. The sample excitation (514.5 nm Ar<sup>+</sup> line) and photoluminescence collection were provided by an optical fiber.

The Darwin-Fock states in the dots were analyzed by the single particle Luttinger-Kohn method [7–9] as well as by the effective mass many-electron many-hole Hartree-Fock method, whereas the influence of the direct and exchange Coulomb interaction on the magnetic dispersion of luminescence as a function of the number of confined carriers was studied by the Hartree-Fock method. The total many particle wave function is a direct product of the electron and the hole Slater determinants with single electron and single hole orbitals  $\psi_\nu^e(\mathbf{r}, \sigma_\nu) = \phi_\nu^e(\mathbf{r})\chi_{\sigma_\nu} = R_{n_\nu, |m_\nu|}^e(r, z)e^{im_\nu\phi}\chi_{\sigma_\nu}$  and  $\psi_\mu^{hh}(\mathbf{r}, \sigma_\mu) = \phi_\mu^{hh}(\mathbf{r})\chi_{\sigma_\mu} = R_{n_\mu, |m_\mu|}^{hh}(r, z)e^{im_\mu\phi}\chi_{\sigma_\mu}$ , respectively. In the spin-restricted configuration-averaged Hartree-Fock method [10] the single particle orbitals are calculated self-consistently from the coupled eigenvalue equations

$$\left[ f^e(r) - V_C(r) + V_{EX, \nu}^e + \frac{\bar{\omega}^2 r^2}{2m_r^e} \right] \phi_\nu^e(r) = \varepsilon_\nu^e \phi_\nu^e(r) \quad (1)$$

and

$$\left[ f^{hh}(r) + V_C(r) + V_{EX, \mu}^{hh} + \frac{\bar{\omega}^2 r^2}{2m_r^{hh}} \right] \phi_\mu^{hh}(r) = \varepsilon_\mu^{hh} \phi_\mu^{hh}(r). \quad (2)$$

In Eqs. (1) and (2) the single particle effective mass Hamiltonians are given by

$$f^{(e, hh)} = -\frac{\hbar^2}{2} \left[ \left( \frac{\partial}{\partial z} \frac{1}{m_z^{(e, hh)}(r, z)} \frac{\partial}{\partial z} \right) + \frac{1}{r} \frac{\partial}{\partial r} \left( \frac{r}{m_r^{(e, hh)}(r, z)} \frac{\partial}{\partial r} \right) - \frac{1}{m_r^{(e, hh)}} \frac{m^2}{r^2} \right] + V_{QW}^{(e, hh)}(z) + V_{strain}^{(e, hh)}(r, z), \quad (3)$$

where  $V_{QW}^{(e, hh)}(z)$  is the band edge confinement potential and  $V_{strain}^{(e, hh)}(z, r)$  the strain induced deformation potential. The magnetic confinement is included in the diamagnetic term  $\bar{\omega}^2 r^2 / 2m^{e, hh}$ , where  $\bar{\omega} = eB/2$ . The Zeeman splitting given by  $(e\hbar B / 2m_r^{(e, hh)})mB$  and the spin splitting  $(e\hbar B / 2m_0)g_S\sigma B$  do not influence the single particle orbitals and can be added to the total Hartree-Fock energy.

The direct Coulomb interaction (including self-interaction) and the orbital dependent exchange interaction are given by  $V_C(r)$  and  $V_{EX, \nu}^e$ , respectively. The Hartree-Fock single particle energies and orbitals were

calculated for  $N_{e-h} = 2, 6$ , and 8 electron-hole pairs which correspond to closed shell configurations, so that the orthogonality of orbitals is obtained without Lagrange multipliers. The redshifts of the luminescence lines were calculated by using a generalization of the Koopmans theorem for the electron-hole system. We used the 2D continuum of QW states as the origin of our single particle energy scale. According to the Koopmans theorem, with this choice, the Hartree-Fock single particle energies represent the energy needed to ionize a confined carrier from the QD state to the QW continuum with the assumption that the other carriers are not relaxed during the ionization process (frozen core approximation). The redshift of a recombination line is thus given by the sum of the Hartree-Fock single particle energies of the recombining electron and hole.

In Fig. 1 we show the typical evolution of the QD PL spectra under magnetic field perpendicular to the QW layer. The power density was set around 0.1 W cm<sup>-2</sup> so as to have band filling spectra with at least three well resolved transitions corresponding to  $N_{e-h} = 6, 8$  per dot. The photoluminescence of the QW between adjacent dots was recorded under the same experimental conditions in the energy range 1.26–1.38 eV (Fig. 2). With increasing magnetic field flux the excited QD states broaden and split into two or more lines of different amplitude and width, depending on the value of the angular momentum quantum number. For fields higher than 10 T, all the split quantum dot levels merge into two main bands which prelude the formation of the quantum dot Landau levels. Above 20 T a strong band with a broad high energy tail

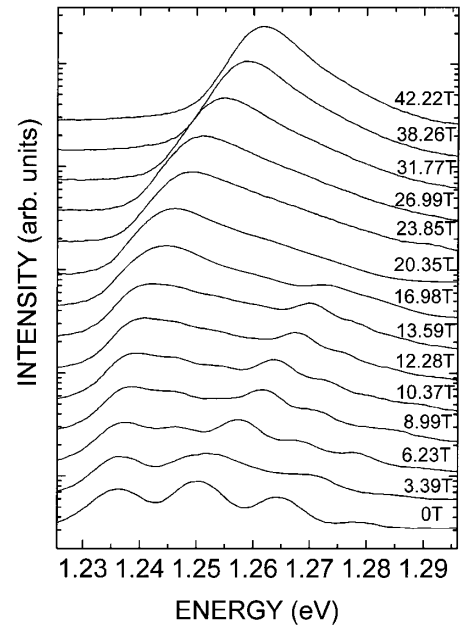


FIG. 1. Magnetoluminescence spectra of the InGaAs strain induced quantum dot sample, in the energy range of the quantum dot emission.

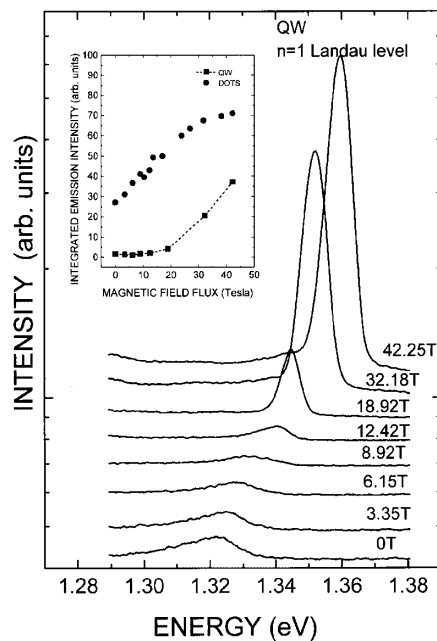


FIG. 2. Magnetoluminescence spectra of the quantum well. Inset: Integrated emission intensities for the quantum dots and quantum well magnetoluminescence.

remains, while the higher energy Landau level disappears and a strong increase of the QW luminescence intensity is observed (see Fig. 2). This is due to the carrier spillover from the higher dot states into the quantum well continuum. The integrated emission intensity of the dots and of the quantum well displayed in the inset of Fig. 2 clearly show the enhancement of the QW emission occurring above 20 T. Moreover, we note that at low fields the integrated QW luminescence intensity is smaller than the intensity of luminescence from QD states, indicating efficient carrier transfer and trapping in the two dimensional parabolic stressor potential.

In order to obtain the complete fan plot of all the transitions, shown in the inset of Fig. 3, we have processed each QD and QW magnetoluminescence spectrum by a Gaussian deconvolution, following the procedure explained in our previous paper [8]. The lifting of degeneracy of the excited states (Zeeman effect) is clearly observable at low fields. At high fields the  $1\Sigma$  state and the states with  $m < 0$  group into the lowest QD Landau level ( $1\Sigma$ ) forming the broad high energy tail of the emission band, whereas the higher energy levels ( $n\Sigma$ , with  $n > 1$  or states with  $m > 0$ ) spillover into the lowest QW Landau level. For fields higher than 20 T, the broadening of the PL bands compares to the splitting between the  $1\Sigma^{\downarrow}$  and the  $1\Pi^{-1}$  lines. All the other  $m < 0^{\downarrow}$  branches fall between these two transitions, and cannot be resolved individually due to the small energy separation (less than 3 meV) [11].

Let us now discuss the comparison between the experimental fan plot and the calculated diamagnetic shifts. In Ref. [8] we showed that a single particle four band model

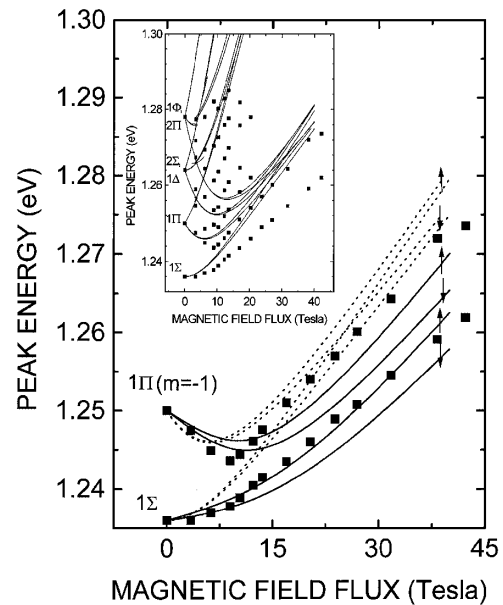


FIG. 3. Comparison between the experimental diamagnetic shift of the ground Landau level (consisting of the  $1\Sigma$  and  $m < 0$   $1\Pi$  transitions), and the theoretical shift calculated in the single particle approximation (dotted curves) or in the full Hartree-Fock model taking into account the electron-hole correlation effects (continuous curves). The symbols  $\uparrow$  and  $\downarrow$  on the curves indicate the spin orientation. Inset: Comparison between the experimental data (symbols) and the calculated (lines) single-particle magnetic field dependence of the ground ( $1\Sigma$ ) and excited ( $1\Pi$ ,  $2\Sigma$ ,  $2\Pi$ ) quantum dot states.

describes the diamagnetic shift and the Zeeman splitting of the parabolic quantum dots for magnetic field fluxes up to 10 T. In the present experiment, we find that the single particle model fails above 10 T, i.e., when the magnetic confinement becomes comparable to the strain induced potential. Therefore it is no longer possible to neglect the electron-electron, electron-hole, and hole-hole interactions which are enhanced in the squeezed carrier states. This is clearly shown in Fig. 3, where the single particle diamagnetic shift of the  $1\Sigma$  and  $1\Pi$  states overestimates the experiment by a steadily increasing amount, for field strengths higher than 20 T (dashed lines).

The description of the experimental data improves substantially if we take into account the effects of electron-electron and electron-hole correlation evaluated in the Hartree-Fock approximation [Eqs. (1)–(3)]. The calculated total diamagnetic shift (continuous lines in Fig. 3) reproduces the experimental shift also at very high fields, as opposed to the single particle model (dashed lines). Even the increasing separation of the  $1\Pi$  and  $1\Sigma$  states observed in the experiment for large fields is consistently reproduced by the HF calculations, in contrast to the single particle calculations which forecast an unphysical convergence of the states. The overall decrease of the electron-hole pair energy due to correlation effects amounts to approximately 20 meV at 40 T, i.e., larger than the interband splitting of

the confined states of the dots, and reduces approximately like  $\Delta E \approx -0.5 \text{ meV/T}$ .

The present Hartree-Fock calculations extend up to  $N_{e-h} = 8$ . This is the maximum number of carriers that is computationally feasible using the present algorithm. A comparison between calculations including 6 and 8 electron-hole pairs indicates that the combined direct and exchange Coulomb effect saturates with increasing the number of confined carriers. The many body correction on the higher levels is unfortunately more difficult to be evaluated due to the increasing number of mutual  $e-e$  and  $e-h$  interactions occurring in the higher index subbands having larger degeneracy. However, if we reduce the single particle shift of the excited states by the magnetic field dependent electron-hole correlation energy of the  $1\Sigma^{\uparrow}$  state ( $\Delta E \approx -0.5 \text{ meV/T}$ ), the fan plot in the inset of Fig. 3 interpolates better the experimental data also for the  $1\Delta$ ,  $2\Sigma$ ,  $2\Pi$ , and  $1\Phi$  states. This procedure, though very rough, provides a useful indication about the role of the  $e-h$  correlation on the high energy quantum dot states. It is worth noting that this is the first magnetoluminescence experiment performed at 4 K which well evidences the correlation effects in the optical transition spectra of strongly confined “neutral” quantum dots. Other experiments evidencing the modification of the quantum dot states in magnetic field due to correlation effects have been performed in weakly confined electron systems (typical confinement energy of the order of  $\hbar\omega \approx 3 \text{ meV}$ ) at temperatures of the order of a few hundreds of mK [4,5].

In conclusion, we have investigated the effect of high magnetic fields on the optical properties of strain induced QDs. We found that a single particle picture accounts well for the measured Zeeman splitting and diamagnetic shift of the interband transitions for fields smaller than 10 T. For higher fields electron-hole correlation must be taken into account in order to reproduce the ob-

served shift. The combined effect of direct and exchange Coulomb interaction indeed reduces the total shift at 40 T by about 50% (about 20 meV).

One of the authors (R.C.) acknowledges the hospitality at Tokyo University during the experiments.

- 
- [1] R. Rinaldi *et al.*, Phys. Rev. Lett. **77**, 342 (1996); R. Rinaldi, Int. J. Mod. Phys. B **12**, 471 (1998).
  - [2] C. G. Darwin, Proc. Cambridge Philos. Soc. **27**, 86 (1930).
  - [3] V. Fock, Z. Phys. **47**, 446 (1928).
  - [4] R. C. Ashoori, H. L. Stormer, J. S. Weiner, L. N. Pfeiffer, K. W. Baldwin, and K. W. West, Phys. Rev. Lett. **71**, 613 (1993).
  - [5] S. Tarucha, D. C. Austing, T. Honda, R. J. van der Hage, and L. P. Kouwenhoven, Phys. Rev. Lett. **77**, 3613 (1996).
  - [6] H. Lipsanen, M. Sopenan, and J. Ahopelto, Solid State Electron. **40**, 601 (1996).
  - [7] M. Braskén, M. Lindberg, and J. Tulkki, Phys. Rev. B **55**, 9275 (1997).
  - [8] R. Rinaldi, R. Mangino, R. Cingolani, H. Lipsanen, M. Sopenan, J. Tulkki, and J. Ahopelto, Phys. Rev. B **57**, 9763 (1998).
  - [9] Because of the axial symmetry, the  $z$  component of the total angular momentum  $J_{\text{tot}} = S_z + L_z$  is a constant of motion for both electrons and holes. Thus the single particle carrier states can be labeled by  $n\Sigma_{\uparrow\downarrow}^{\pm}$ ,  $n\Pi_{\uparrow\downarrow}^{\pm}$ ,  $n\Delta_{\uparrow\downarrow}^{\pm}$ ,  $\dots$ , where we use  $\Sigma$ ,  $\Pi$ ,  $\Delta$ ,  $\Phi$ ,  $\dots$ , for quantum number  $m = 0, \pm 1, \pm 2, \pm 3, \pm 4, \dots$ ,  $n$  is the principal quantum number, and  $\uparrow$  ( $\downarrow$ ) indicates the spin up (down).
  - [10] *Introduction to Computational Chemistry* (Wiley, Chichester, 1999).
  - [11] The experimental data points reported in the fan plot of Fig. 3 above 20 T correspond to the  $1\Sigma$  and  $1\Pi^-$  transitions. All the other  $m < 0$  lines merge into the broadening of these two lines.